

Ion-irradiation-induced amorphization of $\text{La}_2\text{Zr}_2\text{O}_7$ pyrochloreJ. Lian,¹ X. T. Zu,^{1,*} K. V. G. Kutty,² J. Chen,¹ L. M. Wang,¹ and R. C. Ewing^{1,3,†}¹*Department of Nuclear Engineering and Radiological Sciences, University of Michigan, Ann Arbor, Michigan 48109-2014*²*Materials Chemistry Division, Indira Gandhi Center for Atomic Research, Kalpakkam, 603 102, India*³*Department of Materials Science & Engineering, University of Michigan, Ann Arbor, Michigan 48109-2104*

(Received 16 April 2002; published 20 August 2002)

The isometric pyrochlore structure, $A_2B_2O_7$, is generally susceptible to radiation damage, but certain compositions are remarkably resistant to radiation damage. In the binary system $\text{Gd}_2(\text{Ti}_{2-x}\text{Zr}_x)\text{O}_7$, the radiation resistance increases dramatically with the substitution of Zr for Ti, until the pure end member $\text{Gd}_2\text{Zr}_2\text{O}_7$ cannot be amorphized, even at doses as high as ~ 100 dpa. Although zirconate pyrochlores are generally considered to be radiation resistant, we report results for the amorphization of a zirconate pyrochlore $\text{La}_2\text{Zr}_2\text{O}_7$ by ion beam irradiation (~ 5.5 dpa at room temperature). The critical amorphization temperature T_c is low, ~ 310 K. The susceptibility to ion-beam-induced amorphization and structural disordering for zirconate pyrochlores is related to the structural deviation from the ideal fluorite structure, as reflected by the x parameter of the O_{48f} .

DOI: 10.1103/PhysRevB.66.054108

PACS number(s): 61.82.-d, 61.80.Jh, 72.80.Ng, 81.40.Wx

Very recently,¹⁻⁹ there has been considerable interest in the response of the pyrochlore structure type to radiation effects. Pyrochlore has a remarkable range of compositions, more than 500 distinct combinations of A - and B -site chemistries,¹⁰⁻¹² which display an unusual variety of physical, chemical, and electronic properties.¹⁰ The properties of pyrochlore, e.g., ionic conductivity, can be manipulated on a nanometer scale by the use of ion-beam irradiation or implantation techniques. The use of ion-beam technologies to manipulate the ionic conductivity of titanate pyrochlore has allowed the fabrication of nanocomposite ionic conductors.¹³ However, the exploitation of the use of ion-beam irradiations to manipulate the properties of the pyrochlore structure requires an understanding of the effect of composition on the cation and anion disordering process. For most pyrochlore compositions, the structure initially disorders to a defect fluorite structure type and then becomes fully amorphous at doses less than 0.5 dpa (Refs. 2, 6, 14, and 15); however, zirconate pyrochlores retain the defect fluorite structure to extremely high doses, ~ 15 dpa at room temperature.¹⁶

Pyrochlore, ideally $A_{1-2}B_2O_6Y_{0-1}$ (typically, A^{2+} or $3+$ are rare earths and actinides; B^{5+} or $4+ = \text{Ti, Zr, Hf, Sn, or Pb}$), is a derivative of the fluorite structure except there are two cation sites and one-eighth of the anions are absent, ideally $(A,B)_4O_7$. The cations at the A and B sites and the oxygen vacancies may be ordered or disordered either by thermal treatment,^{10,17} due to chemical substitution^{10,17,18} or by irradiation.^{4,13-15} The radiation “resistance” depends critically on the ability of the structure to sustain cation disorder on the A and B sites, as well as on a disordering of the oxygen vacancies. The radiation resistance of the $\text{Gd}_2(\text{Ti}_{2-x}\text{Zr}_x)\text{O}_7$ binary system^{2,16} has attracted special attention because pyrochlore can incorporate Pu (Refs. 19 and 20) and be used as a waste form for the immobilization of Pu from dismantled nuclear weapons.^{2,21,22} *In situ* ion-beam irradiation¹⁵ has shown that $\text{Gd}_2\text{Ti}_2\text{O}_7$ is readily amorphized at a low dose (~ 0.18 dpa) by 1-MeV Kr^+ at room temperature, consistent with the dose of $\text{Gd}_2\text{Ti}_2\text{O}_7$ doped with ²⁴⁴Cm, an alpha emitter.²³ However, zirconate pyrochlore, $\text{Gd}_2\text{Zr}_2\text{O}_7$, has a dramatically higher radiation resistance to

ion-beam-induced amorphization and remains crystalline at a dose of 5 dpa (1-MeV Kr^+ at 25 K).^{16,24} Similarly, the $\text{Er}_2\text{Zr}_2\text{O}_7$, which has a disordered defect fluorite structure, is radiation resistant and remains crystalline to a high dose of ~ 140 dpa (5×10^{16} ions/cm² by 350-KeV Xe^+ at room temperature).^{1,9} In contrast, the ordered pyrochlore, $\text{Er}_2\text{Ti}_2\text{O}_7$, becomes amorphous at a dose of only ~ 0.26 dpa.

A number of studies²⁵⁻²⁷ have focused on the theoretical simulation of defect formation in the pyrochlore structure either by energy minimization or modern potential methods, with the goal of understanding the greater radiation stability of zirconate pyrochlores. Simulations have focused on the energetics of A - and B -site cation disordering and its effect on oxygen vacancy disordering. Chartier *et al.*²⁷ have shown that $\text{La}_2\text{Zr}_2\text{O}_7$ has a greater tendency toward cation disorder that decreases with increasing Ti content. From the pure end-member zirconate up to the end-member titanate composition, there is a calculated $\sim 26\%$ increase in the cation antisite formation energy. For the end-member $\text{La}_2\text{Zr}_2\text{O}_7$, an increase in the structural disorder (e.g., La-Zr exchange) causes the calculated cation antisite defect energy to be lowered from 2 to 1.5 eV. Thus the disordered form is energetically favored. These theoretical simulations suggest that $\text{La}_2\text{Zr}_2\text{O}_7$ should be more “resistant” to radiation damage by simply disordering to the defect fluorite structure rather than becoming amorphous.

We have investigated the radiation response of zirconate pyrochlores as a function of different A -site cation compositions $A_2\text{Zr}_2\text{O}_7$ ($A = \text{La, Nd, Sm, and Gd}$), under a 1.5-MeV Xe^+ irradiation using *in situ* TEM observation. Furthermore, a 200-KeV Ti ion implantation on bulk $\text{Gd}_2\text{Zr}_2\text{O}_7$ was conducted to an extremely high ion dose (1×10^{17} ions/cm²), and the microstructural evolution was studied using cross-sectional TEM techniques.

Samples were prepared by a sol-gel method with an aqueous mixture of zirconyl chloride solutions and the appropriate rare-earth nitrate. These solutions were mixed and treated with equal volumes of semimolar aqueous solutions of citric acid and ethylene glycol. The mixture was evaporated to dryness to form a porous resin mass. This precursor was

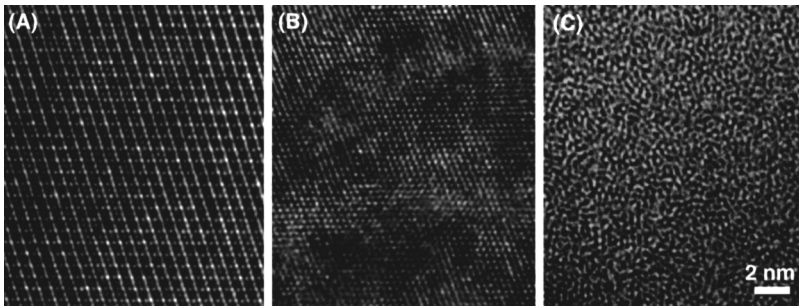


FIG. 1. (A) An ordered pyrochlore structure for unirradiated zirconate. (B) Highly radiation resistant disordered defect fluorite structure of irradiated $\text{Gd}_2\text{Zr}_2\text{O}_7$ at a dose of ~ 36 dpa at 25 K. Ion irradiation-induced disorder fluorite is evidenced by the loss of superstructure as compared with the ordered pyrochlore (A). (C) Completely amorphous structure in $\text{La}_2\text{Zr}_2\text{O}_7$ irradiated by 1.5-MeV Xe^+ at a dose of ~ 5.5 dpa at room temperature.

calcined at 700 °C for 15 min, and the final heat treatment was at 1400 °C in air for 10–30 h. For $\text{Gd}_2\text{Zr}_2\text{O}_7$, the calcine was sintered at 1600 °C for 50 h in air, and the material tends to adopt a closely related anion deficient fluorite structure due to a thermally induced pyrochlore-to-fluorite transition. The pyrochlore superstructures of $\text{La}_2\text{Zr}_2\text{O}_7$, $\text{Gd}_2\text{Zr}_2\text{O}_7$, $\text{Sm}_2\text{Zr}_2\text{O}_7$, and $\text{Nd}_2\text{Zr}_2\text{O}_7$ were confirmed by transmission electron microscopy [Fig. 1(A)], and all zirconate samples were stable under 200- and 400-KeV electron-beam irradiations. The 1.5-MeV Xe^+ ion irradiation and *in situ* TEM observation were performed using the HVEM-Tandem Facility at the Argonne National Laboratory over a temperature range of 25–300 K, and the ion flux was 8.6×10^{11} ions/cm²/s. The structural damage upon irradiation was monitored by the selected area electron diffraction patterns (SAED) under *in situ* TEM observations. The critical amorphization dose D_c was determined as the ion dose at which complete amorphization occurs, as manifested by the disappearance of all diffraction maxima in the SAED patterns. Ti-ion implantation of the bulk $\text{Gd}_2\text{Zr}_2\text{O}_7$ sample was conducted using a Varian 200 ion implanter at room temperature. The microstructural evolution upon ion irradiation and implantation was studied by *ex situ* high-resolution transmission electron microscope (HRTEM) and cross-sectional TEM.

All of the zirconate pyrochlore compositions displayed an ion irradiation-induced pyrochlore-to-defect fluorite structural transformation, as has been reported for $\text{Gd}_2\text{Ti}_2\text{O}_7$.^{13,15} The diffraction maxima from the superstructure of the ordered pyrochlore lattice disappeared gradually with increasing ion dose as observed from *in situ* TEM. For $\text{Gd}_2\text{Zr}_2\text{O}_7$, $\text{Sm}_2\text{Zr}_2\text{O}_7$, and $\text{Nd}_2\text{Zr}_2\text{O}_7$, the defect fluorite structure was radiation resistant, and complete amorphization could not be achieved under Xe^+ irradiation at 25 K [Fig. 1(B)]. The $\text{Gd}_2\text{Zr}_2\text{O}_7$ was also irradiated to a dose of 1×10^{17} ions/cm² at room temperature with 200-keV Ti^+ . A highly damaged layer was created by ion implantation with a thickness of ~ 150 nm. The SAED insets [Fig. 2(B)] and HRTEM image [Fig. 2(D)] indicate the occurrence of ion implanted-induced pyrochlore-to-fluorite structural transition, as evidenced by the disappearance of superstructure in both diffraction patterns and the HREM image. Based on the damage profile calculated by SRIM-2000,²⁸ employing 50 eV as the displacement energy (E_d), a peak damage level of ~ 100 dpa was obtained. The disordered defect fluorite structure of $\text{Gd}_2\text{Zr}_2\text{O}_7$ is thus extremely stable under very high dose irradiations.

In contrast, for $\text{La}_2\text{Zr}_2\text{O}_7$, the ion-irradiation-induced

order-disorder transformation occurred simultaneously with the amorphization process; and with increasing ion dose, the defect fluorite structure amorphized. Above the critical amorphization dose D_c (~ 5.5 dpa at room temperature), the diffraction maxima from the crystalline defect fluorite structure disappeared completely, and the fully amorphous state was achieved as confirmed by a HRTEM image [Fig. 1(C)]. The temperature dependence of the critical amorphization dose for $\text{La}_2\text{Zr}_2\text{O}_7$ irradiated by 1.5-MeV Xe^+ is shown in Fig. 3. The critical amorphization dose increases at elevated irradiation temperatures, and eventually, complete amorphization cannot be attained even at high ion doses above this critical temperature.

The temperature dependence of amorphization is a result of the competition between amorphization and recovery processes. Based on a cascade-quenching model,²⁹ the main recovery mechanism in the irradiation-induced amorphization process is epitaxial recrystallization at the interface of the crystalline/amorphous region around the cascade. Wang, Wang, and Ewing³⁰ have presented a model to describe the temperature dependence of amorphization using the concept of recrystallization efficiency, A , the volume fraction recrystallized within a single cascade. The experimental data are fitted using a temperature-dependent amorphization dose function, and the critical amorphization temperature T_c for $\text{La}_2\text{Zr}_2\text{O}_7$ was determined to be ~ 310 K with an activation

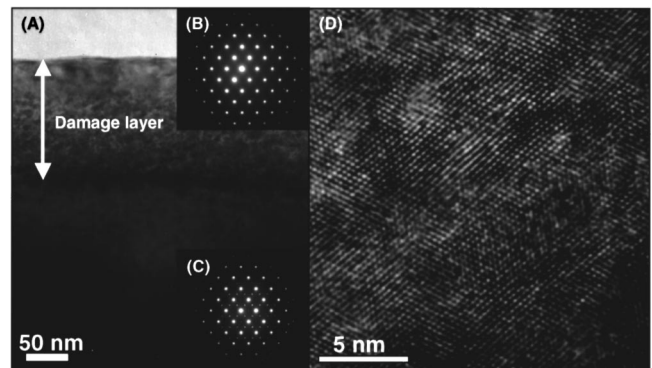


FIG. 2. (A) Cross-sectional TEM image of $\text{Gd}_2\text{Zr}_2\text{O}_7$ implanted by 200-keV Ti ions at room temperature to a dose of 1×10^{17} ions/cm² (~ 100 dpa). A highly damaged layer is created with a thickness of ~ 150 nm. Insets are SAED diffraction patterns from the damaged layer (B) and the substrate (C). The loss of superstructure in both the diffraction pattern (B) and the HRTEM image (D) of highly damaged layer suggests a disordered fluorite structure formed upon ion implantation.

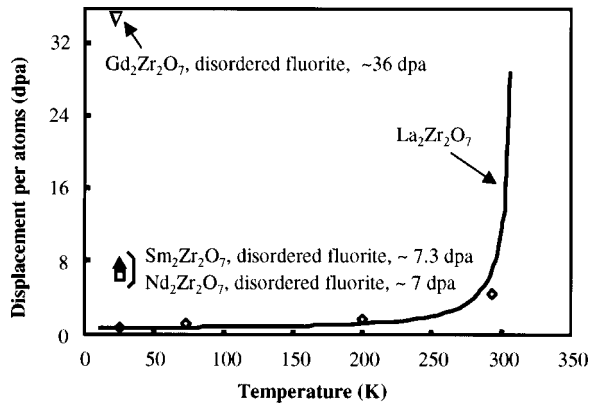


FIG. 3. Temperature dependence of critical amorphization dose of $\text{La}_2\text{Zr}_2\text{O}_7$ irradiated by 1.5-MeV Xe^+ . The temperature dependence curve of $\text{La}_2\text{Zr}_2\text{O}_7$ is obtained by fitting the experimental data based on the model presented in Ref. 30. The critical amorphization temperature T_c is determined to be ~ 310 K, and above this temperature complete amorphization cannot occur. The irradiation results for $\text{Gd}_2\text{Zr}_2\text{O}_7$, $\text{Sm}_2\text{Zr}_2\text{O}_7$, and $\text{Nd}_2\text{Zr}_2\text{O}_7$ are included for comparison, although none of these compositions is amorphized.

energy of 0.05 eV. From the temperature dependence curve of $\text{La}_2\text{Zr}_2\text{O}_7$, the critical amorphization dose increases with temperature, and, above the critical amorphization temperature, complete amorphization cannot occur. Depending on the models employed, one may obtain quite different values for the activation energy. Thus T_c is a more useful parameter for comparing the radiation resistant of phases to ion-beam-induced amorphization.

The substitution of La^{3+} for Gd^{3+} at the A site of pyrochlore has a significant effect on the irradiation behavior of rare-earth zirconate pyrochlores (Fig. 3). $\text{Gd}_2\text{Zr}_2\text{O}_7$ is highly radiation resistant; in contrast, $\text{La}_2\text{Zr}_2\text{O}_7$ is the only zirconate pyrochlore that has been amorphized by ion beam irradiation. Table I summarizes the radiation response of lanthanide zirconate pyrochlores as a function of the A- and B-cation radius ratios, which can be used to define the stability field of the pyrochlore superstructure,¹⁰ and the x parameter of 48f oxygen, which can be used to describe the shapes of the coordination polyhedra in the pyrochlore structure. With the systematic decrease in the average A- to B-cation radius ratio there is a tendency to cation disordering of the pyrochlore that leads to a disordered defect fluorite structure, $(A,B)_4\text{O}_7$.^{4,10,17} $\text{Gd}_2\text{Zr}_2\text{O}_7$ is near the boundary between the ordered pyrochlore vs the disordered defect

fluorite structure type. Typical radius ratios for ordered pyrochlores are between 1.46 ($\text{Gd}_2\text{Zr}_2\text{O}_7$) and 1.78 ($\text{Sm}_2\text{Ti}_2\text{O}_7$). Disordered, defect fluorite structures can form when the cation radius ratio is below 1.46 (e.g., $\text{Gd}_2\text{Zr}_2\text{O}_7$ and $\text{Er}_2\text{Zr}_2\text{O}_7$). The x parameter of the 48f oxygen can be used to describe the deviation of the pyrochlore structure from an ideal fluorite structure (for which the A-site cation is in perfect cubic coordination). For a perfectly ordered pyrochlore, the x parameter is 0.3125 (the B-site cation is in perfect octahedral coordination); whereas, for $x=0.375$, the structure becomes an ideal fluorite structure.¹⁰ From the irradiation results and the corresponding x parameter, a close correlation exists between the resistance to ion-irradiation-induced amorphization and the deviation from the ideal fluorite structure and the related tendency toward an order-disorder transition. $\text{La}_2\text{Zr}_2\text{O}_7$ has an ordered pyrochlore structure ($x=0.333$) and the largest deviation from an ideal fluorite structure ($x=0.375$), as evidenced by the fact that it has the smallest x parameter for the 48f oxygen (Table I). As a result, $\text{La}_2\text{Zr}_2\text{O}_7$ has the greatest susceptibility to radiation damage among the rare-earth zirconate pyrochlores. In contrast, $\text{Gd}_2\text{Zr}_2\text{O}_7$ has a structure that is essentially the same as that of stabilized cubic zirconia, which remains crystalline under Xe^{2+} irradiation up to 680 dpa.³¹ Thus, $\text{Gd}_2\text{Zr}_2\text{O}_7$ adopts a disordered defect fluorite structure that does not amorphize²⁵⁻²⁷ and has a high resistance to ion irradiation-induced amorphization.

Using both classical potential and *ab initio* methods, Chartier *et al.*²⁷ have modeled the influence of structural disordering and the order-disorder transition on the radiation response of the $\text{La}_2\text{Zr}_{2(1-y)}\text{Ti}_y\text{O}_7$ system. They concluded that under irradiation, cation antisite defects occur, consistent with previous theoretical results.^{1,25,26} The cation antisite is enhanced with the increasing degree of structural disordering by lowering the cation antisite formation energy (e.g., 2 eV for ordered $\text{La}_2\text{Zr}_2\text{O}_7$ and 1.5 eV with coupled switching of La and Zr), and the vacant 8a oxygen site becomes increasingly occupied. Their results indicate that $\text{La}_2\text{Zr}_2\text{O}_7$ has a tendency toward cation disordering, but with the addition of Ti, the tendency toward cation disordering is less energetically favorable in the $\text{La}_2\text{Zr}_{2(1-y)}\text{Ti}_y\text{O}_7$ system. This is confirmed by a systematic irradiation study of compositions in the $\text{Gd}_2\text{Zr}_x\text{Ti}_{1-x}\text{O}_7$ system,¹⁶ where materials show a gradually increasing resistance to ion-irradiation-induced amorphization with the increasing Zr contents. This reflects a reduction in the energetic barrier to the order-disorder transition.

TABLE I. The structural parameters (cation radius ratios and x parameters for the 48f oxygen) and the radiation response of zirconate pyrochlores to a 1.5-MeV Xe^+ irradiation.

Phase	Structure	r_A/r_B	x parameter for 48f oxygen	T_c (K)
$\text{La}_2\text{Zr}_2\text{O}_7$	pyrochlore	1.61	0.333	310
$\text{Nd}_2\text{Zr}_2\text{O}_7$	pyrochlore	1.54	0.335	defect fluorite
$\text{Sm}_2\text{Zr}_2\text{O}_7$	pyrochlore	1.50	0.342	defect fluorite
$\text{Gd}_2\text{Zr}_2\text{O}_7$	pyrochlore/fluorite	1.46	0.345	defect fluorite

Our results confirm the theoretical calculations. We have shown the extremely high resistance of $\text{Gd}_2\text{Zr}_2\text{O}_7$ to ion-beam-induced amorphization (to a dose of approximately 100 dpa). While, for $\text{La}_2\text{Zr}_2\text{O}_7$, there is an initial stage of cation disordering under irradiation as predicted by Chartier *et al.*,²⁷ however, this ion-irradiation-induced disordered state is unstable with respect to the amorphous state that forms at higher doses. The increasing resistance to ion-irradiation-induced amorphization for zirconate pyrochlore as *A*-site cations become smaller (e.g., La^{3+} to Gd^{3+}) emphasizes the importance of structural controls. The greater the deviation from the ideal fluorite structure type ($x_{48f} = 0.375$), the more susceptible the pyrochlore is to radiation damage (and the greater the energetic barrier to disordering).

The relationship between the resistance to ion-irradiation-induced amorphization (the stability of defect fluorite) and the energetics of the order-disorder transition is analogous to that of thermally induced order-disorder structural transformations in pyrochlore. The order-disorder transformation of the pyrochlore-to-fluorite transformation has also been observed for zirconate pyrochlores $A_2\text{Zr}_2\text{O}_7$ ($A = \text{Nd}, \text{Sm}, \text{Gd}$) as a result of disordering by thermal treatment. The transition temperatures for Gd, Sm, and Nd zirconate pyrochlores are 1550, 2200, and 2300 °C, respectively.^{10,17} The more similar

the structure is to ideal fluorite, the greater the tendency toward structural disordering, and the more stable the defect fluorites is with respect to the ordered pyrochlore state.

In summary, the resistance of $A_2\text{Zr}_2\text{O}_7$ pyrochlores ($A = \text{La}, \text{Nd}, \text{Sm}, \text{and Gd}$) to radiation damage varies with *A*-site cation composition. The high radiation resistance for $\text{Gd}_2\text{Zr}_2\text{O}_7$ is further confirmed by a 1.5-MeV Xe^+ irradiation at 25 K and 200-keV Ti-ion implantation at room temperature; while $\text{La}_2\text{Zr}_2\text{O}_7$ is the only zirconate pyrochlore that has been amorphized by ion-beam irradiation. The susceptibility to ion-beam damage for pyrochlore compounds is closely related to the deviation from the ideal fluorite structure, as represented by the x parameter for the 48*f* oxygen. Pyrochlores that are structurally close to the fluorite structure (e.g., $x = 0.375$) have a greater tendency toward order-disorder transition and are more resistant to ion-beam-induced amorphization.

The authors thank the staff of HVEM-Tandem Facility at Argonne National Laboratory for assistance during ion irradiation experiments and V. H. Rotberg for conducting the ion implantation. This work was supported by the Office of Basic Energy Sciences, U.S. Department of Energy under Grant No. DE-FG02-97ER45656.

*Present address: Department of Physics, Sichuan University, Chengdu 610064, Peoples Republic of China.

†Author to whom correspondence should be addressed. Email address: rodewing@umich.edu

¹K. E. Sickafus, L. Minervini, R. W. Grimes, J. A. Valdez, M. Ishimaru, F. Li, K. J. McClellan, and T. Hartmann, *Science* **289**, 748 (2000).

²W. J. Weber and R. C. Ewing, *Science* **289**, 2051 (2000).

³R. C. Ewing, A. Meldrum, L. M. Wang, and S. X. Wang, in *Transformation Processes in Minerals*, edited by S. A. T. Redfern and M. A. Carpenter, *Reviews in Mineralogy & Geochemistry* No. 39 (Mineralogical Society of America and Geochemical Society, Washington, 2000), p. 319.

⁴B. D. Begg, N. J. Hess, W. J. Weber, R. Devanathan, J. P. Icenhower, S. Thevuthasan, and B. P. McGrail, *J. Nucl. Mater.* **288**, 208 (2001).

⁵G. R. Lumpkin, K. L. Smith, and M. G. Blackford, *J. Nucl. Mater.* **289**, 177 (2001).

⁶B. D. Begg, N. J. Hess, D. E. McCready, S. Thevuthasan, and W. J. Weber, *J. Nucl. Mater.* **289**, 188 (2001).

⁷A. Meldrum, C. W. White, V. Keppens, L. A. Boatner, and R. C. Ewing, *Phys. Rev. B* **63**, 104109 (2001).

⁸J. Chen, J. Lian, L. M. Wang, R. C. Ewing, and L. A. Boatner, *Appl. Phys. Lett.* **79**, 1989 (2001).

⁹K. E. Sickafus, L. Minervini, R. W. Grimes, J. A. Valdez, and T. Hartmann, *Radiat. Eff. Defects Solids* **155**, 133 (2001).

¹⁰A. Subramanian, G. Aravamudan, and G. V. S. Rao, *Prog. Solid State Chem.* **15**, 55 (1983).

¹¹B. C. Chakoumakos, *J. Solid State Chem.* **53**, 120 (1984).

¹²G. R. Lumpkin, R. C. Ewing, C. T. Williams, and A. N. Mariano, in *Scientific Basis for Nuclear Waste Management XXIV*, edited by K. P. Hart and G. R. Lumpkin, *MRS Symposia Proceedings* No. 663 (Materials Research Society, Pittsburgh, 2001), p. 921.

¹³J. Lian, L. M. Wang, S. X. Wang, J. Chen, L. A. Boatner, and R. C. Ewing, *Phys. Rev. Lett.* **87**, 145901 (2001).

¹⁴S. X. Wang, L. M. Wang, R. C. Ewing, and K. V. G. Kutty, *Nucl. Instrum. Methods Phys. Res. B* **169**, 135 (2000).

¹⁵S. X. Wang, L. M. Wang, R. C. Ewing, G. S. Was, and G. R. Lumpkin, *Nucl. Instrum. Methods Phys. Res. B* **148**, 704 (1999).

¹⁶S. X. Wang, B. D. Begg, L. M. Wang, R. C. Ewing, W. J. Weber, and K. V. G. Kutty, *J. Mater. Res.* **14**, 4470 (1999).

¹⁷B. J. Wuensch and K. W. Eberman, *JOM* **52**, 19 (2000).

¹⁸C. Heremans, B. J. Wuensch, J. K. Stalick, and E. Prince, *J. Solid State Chem.* **117**, 108 (1995).

¹⁹N. K. Kulkarni, S. Sampath, and V. Venugopal, *J. Nucl. Mater.* **281**, 248 (2000).

²⁰S. Yamazaki, T. Yamashita, T. Matsui, and T. Nagasaki, *J. Nucl. Mater.* **294**, 183 (2001).

²¹W. J. Weber, R. C. Ewing, C. R. A. Catlow, T. D. de la Rubia, L. W. Hobbs, C. Kinoshita, H. Matzke, A. T. Motta, M. Nastasi, E. K. H. Salje, E. R. Vance, and S. J. Zinkle, *J. Mater. Res.* **13**, 1434 (1998).

²²R. C. Ewing, *Can. Mineral.* **39**, 697 (2001).

²³W. J. Weber, J. W. Wald, and H. J. Matzke, *J. Nucl. Mater.* **138**, 196 (1986).

²⁴S. X. Wang, L. M. Wang, R. C. Ewing, and K. V. Govindan Kutty, in *Microstructural Processes in Irradiated Materials*, edited by S. J. Zinkle, G. E. Lucas, R. C. Ewing, and J. S. Williams, *MRS Symposia Proceedings* No. 540 (Materials Research Society, Pittsburgh, 1999), p. 355.

²⁵R. E. Williford, W. J. Weber, R. Devanathan, and J. D. Gale, *J. Electroceram.* **3**, 409 (1999).

²⁶L. Minervini, R. W. Grimes, and K. E. Sickafus, *J. Am. Ceram. Soc.* **83**, 1873 (2000).

²⁷A. Chartier, C. Meis, W. J. Weber, and L. R. Corrales, *Phys. Rev. B* **65**, 134116 (2002).

- ²⁸J. F. Ziegler, J. P. Biersack, and U. Littmark, *The Stopping and Range of Ions in Solids* (Pergamon, New York, 1985).
- ²⁹W. J. Weber, Nucl. Instrum. Methods Phys. Res. B **166**, 98 (2000).
- ³⁰S. X. Wang, L. M. Wang, and R. C. Ewing, Phys. Rev. B **63**,

024105 (2001).

- ³¹K. E. Sickafus, H. Matzke, T. Hartmann, K. Yasuda, J. A. Valdez, P. Chodak, M. Nastasi, and R. A. Verrall, J. Nucl. Mater. **274**, 66 (1999).